Journal of Alloys and Compounds 978 (2024) 173500

Contents lists available at ScienceDirect

Journal of Alloys and Compounds

journal homepage: www.elsevier.com/locate/jalcom

The relationship between the plasma edge and topological properties of Sb_2Te_3 under pressure

Xu Zheng [a], Xi Wang [a], ZeXiao Zhang [a], Chun Wang [b,c], Bin Hu [c,*], Chan Gao [a], Sa Zhang [a,*], Changqing Jin [b], Xiaohui Yu [b,*]

[a] Department of Physics, Chengdu University of Technology, Chengdu 610059, China
[b] Beijing National Laboratory for Condensed Matter Physics and Institute of Physics, Chinese Academy of Sciences, Beijing 100190, China
[c] Research Institute of Aero-Engine, Beihang University, Xueyuan Road, Beijing 100191, China

ARTICLE INFO

Keywords:
Topological insulators
Plasma edge
High-pressure infrared

ABSTRACT

Topological insulators have garnered considerable attention in recent years due to their unique electronic properties. However, pressure-induced topological materials often located in the middle of the two diamonds and cannot be detected by Angle resolved electron spectra. Such topological materials only stay in theoretical calculated. Since diamond has a high optical transmittance, its optical properties have been extensively studied to probe the band structure of topological insulators under pressure. In this paper, we determine the high-pressure infrared (IR) properties by measuring the transmittivity and reflectivity of Sb_2Te_3 up to 23.2 GPa. The plasma edge shows jumping at 4.2 GPa and 8.5 GPa, where is caused by the change of charge carrier features and a new phase appears at 8.5 GPa. Furthermore, by analyzing the position of plasma edge under pressure, we find that the absence of plasma edge at high pressure corresponds to the disappearance of the Sb_2Te_3 topological structure. Therefore, utilizing the plasma edge to investigate the modification of band structure in materials under high pressures is highly effective.

1. Introduction

In recent years, topological insulators (TIs) have attracted considerable attention due to their novel electronic properties. TIs have topologically protected stable low-dimensional metallic states on their band boundaries, presenting significant potential for applications in spintronics, quantum computation, and thermoelectric energy conversion [1–7]. Most of the proposed TIs are proved by using angle-resolved electron spectroscopy or first-principles calculations [8–10]. Recently, pressure-induced TIs have attracted much attention, as these insulators exhibit unique electronic properties [11–15]. However, since the topological state under high pressure is situated in the middle of two diamonds, it cannot be detected by angle-resolved electron spectroscopy, leaving the band structure characteristics of pressure-induced TIs solely in the realm of theoretical calculations [16,17]. Furthermore, the topological band predicted through theoretical calculations yields inconclusive results, as it is discovered that the band structure is highly sensitive to lattice parameters, making precise calculations challenging.

Due to the high optical transmittivity of diamond, the optical properties have been well studied to probe the band structure of pressure-induced TIs [18,19]. Topologically distinct phases under hydrostatic pressures have been claimed by observing the phonon line-width and carrier characters at the position of topological phase transition under pressure [11,12]. Dordevic et al. revealed the charge inhomogeneities by high pressure infrared spectra of topological insulators [20]. The structural transition and charge dynamics of $TiTe_2$ at high pressure can also be found by using high pressure infrared spectra [21]. Hence, the pressure-induced topological phase and the band structure characters are exactly probed by infrared reflectivity and transmittivity measurements.

The surface of topological insulators exhibits metal-like properties, leading to the presence of plasma on its surface [22–28]. Although high pressure infrared spectra has been used in the study of topological structure transition and charge transfer, its potential in studying surface plasma and assessing topological band structure under high pressure has been overlooked. In 2010, the plasma edge of topological insulators was first discussed at Stanford University [29]. Therefore, we believe that high pressure infrared spectra have the potential to detect the plasma

* Corresponding authors.
E-mail addresses: hubin@buaa.edu.cn (B. Hu), 15136231837@163.com (S. Zhang), xhyu@iphy.ac.cn (X. Yu).

https://doi.org/10.1016/j.jallcom.2024.173500
Received 14 September 2023; Received in revised form 30 December 2023; Accepted 8 January 2024
Available online 9 January 2024

edge of topological insulators and explore the topological band structure characters under high pressure.

In this study, we determine the high pressure infrared properties by measuring transmittivity and reflectivity of Sb_2Te_3 up to 23.2 GPa. The plasma edges exhibit two jumps at 4.2 GPa and 8.5 GPa respectively, which are attributed to a change in carrier characters and a new phase of Sb_2Te_3 appears at 8.5 GPa. Also, through the changes of plasma edges with pressure, we find that the disappearance of plasma edges under high pressure corresponds to the disappearance of topological band structure of Sb_2Te_3. Furthermore, we believe that it is very effective to use plasma edges to study the change of band structure of topological materials under high pressure.

2. Materials and methods

Single crystals of Sb_2Te_3 were grown using Bridgeman's method[30]. Stoichiometric amounts of high purity elements Sb (99.999%) and Te (99.999%) were mixed, ground, and pressed into pills. These pills were then loaded into a quartz Bridgeman ampoule, which was then evacuated and sealed. The ampoule was placed in a furnace and heated at 800 ℃ for 3 days. After that, the ampoule was slowly cooled in 5 ℃/ h.

All measurements were performed on natural, freshly cleaved surfaces to minimize exposure to air. Optical data at high pressure were recorded using a diamond-anvil cell operated in transmission and reflection geometry. A fine dry KBr powder was used as the pressure-transmitting medium, and the pressure was monitored in situ through ruby fluorescence. An overcoating technique, with gold coating of the sample as reference [31], was used to obtain the absolute values of reflectance. Optical data at high pressure were acquired up to 23.2 GPa with type IIa diamond.

All electronic structure calculations are performed with the Vienna Ab-initio Simulation Package (VASP) [32,33] based on density-functional theory, and the spin–orbit coupling (SOC) are considered for Sb_2Te_3.

3. Results and discussion

Infrared spectra of Sb_2Te_3 is reported in Fig. 1 at ambient environment, the insert is a single crystal picture of Sb_2Te_3. Reflectivity spectra were collected along the cleaved surfaces. The results, illustrated in Fig. 1, display a well defined plasma edge at the wavenumber of about 1000 cm^{-1}, consistent with previous reports [20]. In the case of TIs, the

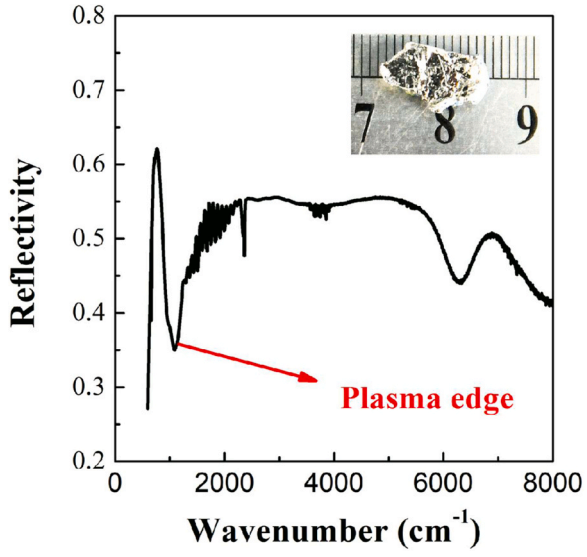

Fig. 1. Reflectivity spectra of Sb_2Te_3 from 600 cm^{-1} to 8000 cm^{-1} at ambient environment, the insert is a single crystal picture of Sb_2Te_3.

helical metal, which possesses metal-like surface properties, holds great significance in regard to the plasmon excitons of TIs. This characteristic shape of reflectivity is a consequence of zero crossing in the real part of the dielectric function [34] that occurs at the so called renormalized plasma frequency:

$$\omega_p^{*2} = \frac{4\pi ne^2}{m^*\epsilon_\infty}$$

Where m^* is the carrier effective mass, n is the carrier density and ϵ_∞ is the high-frequency dielectric function. In other words, the plasma frequency ω_p^{*2} is related to the carrier characteristic. The position of the plasma edge is approximately in 1089 cm^{-1} consistent with previous reports (1045 cm^{-1}) [20]. Optical properties are important to understand the response of a material to incident its band structure. In the past studies of high pressure infrared spectra, the focus is often on using the change of spectral peak to determine the structure transition or using Kramers-Kronig fitting to study the optical conductivity of topological insulator [35,36]. However, despite reports indicating the observation of plasma in the high-pressure infrared spectrum of TIs, the study of the plasma edge in this field is often overlooked. In the following, we discuss the plasma edges of Sb_2Te_3 under pressure in detail.

High pressure infrared spectra of Sb_2Te_3 is reported over a broad range of frequencies and pressure from 1 GPa to 23 GPa as shown in Figs. 2 and 3. In the reflectance infrared spectrum, it is observed that the plasma edges are located at 1089 cm^{-1} and 1110 cm^{-1}, respectively, at the lowest pressures of 1 GPa and 2.3 GPa. As the pressure increases, the location of the plasma edge shifts, but the moving speed is only approximately 10 cm^{-1}/GPa. Fig. 2(a) displays that above 2.3 GPa, the plasma edges undergo a pressure-induced jump. Compared to the two points of low pressure, the plasma edges at 4.2 GPa has a big jump of about 300 cm^{-1}/GPa, where the change is caused by the pressure-tuned changes on carrier density in Sb_2Te_3. When the pressure reached 8.5 GPa and 10.3 GPa, the plasma edges exhibited a further jump, respectively at 2410 cm^{-1} and 2771 cm^{-1}. The jump was not solely due to the transition from p-type to n-type characteristics but also resulted from the emergence of a new phase of Sb_2Te_3 under the specified pressure, known as (Phase I+II) [37]. This mixed phase persisted up to a pressure of 12.3 GPa.

Fig. 2(b) shows experimental results variation in infrared transmittivity of Sb_2Te_3 with pressure, ranging from 1.2 to 10.3 GPa. The diagram reveals that Sb_2Te_3's average transmittance is approximately 0.9 under low pressure, with a gradual upward trend. However, at pressures exceeding 4.2 GPa, the transmittance of Sb_2Te_3 exhibits a downward trend due to changes in carrier density at 4.2 GPa. Moreover, with further the increase of pressure, the transmitavity of Sb_2Te_3 continues to decrease, and the maximum transmittance gradually decreases from 0.6 (4.2 GPa) to about 0.2 (10.3 GPa), due to the decrease in band gap and increase in carrier concentration with increasing pressure.

The infrared spectra from 12.1 GPa to 23.2 GPa are illustrated in Fig. 3. When the pressure reaches 12.1 GPa, the plasma edges become indistinct, but the shape of the curve shows that the band structure of Sb_2Te_3 is modified with pressure. According to the experiment of high pressure XRD by Zhao et al. [38], phase transition exists at 12.1–23.2 GPa. Under pressure of 12.1 GPa and 14.1 GPa, the crystal structure at this pressure is phase II. When the pressure reaches 16.8 GPa, Sb_2Te_3 transforms from phase II to phase III. As can be seen from Fig. 3(a), the reflectivity spectrum of Sb_2Te_3 begins to show an upward trend with wavenumber during the transition of phase III, as opposed to the previous downward trend. Fig. 3(b) displays the transmission spectrum of Sb_2Te_3, revealing that with an increase in pressure to 12.1 GPa, the band gap of Sb_2Te_3 diminishes, leading to an uptick in photoconductivity. Therefore, the reflectivity at this time increases with the increase of pressure, while the transmittivity is almost 0.

Fig. 4 displays the variation of plasma edges with varying pressure. It is observed that below 4.0 GPa, the plasma edges increase with pressure,

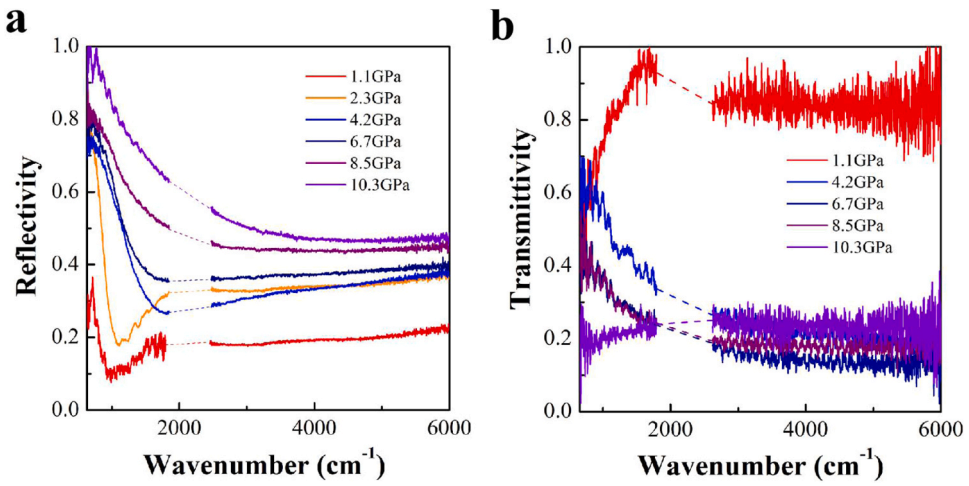

Fig. 2. Infrared spectra of Sb_2Te_3 from 1.1 GPa to 10.3 Gpa. (a) The pressure dependence of reflectivity at different pressure. (b) The pressure dependence of transmittivity at different pressure.

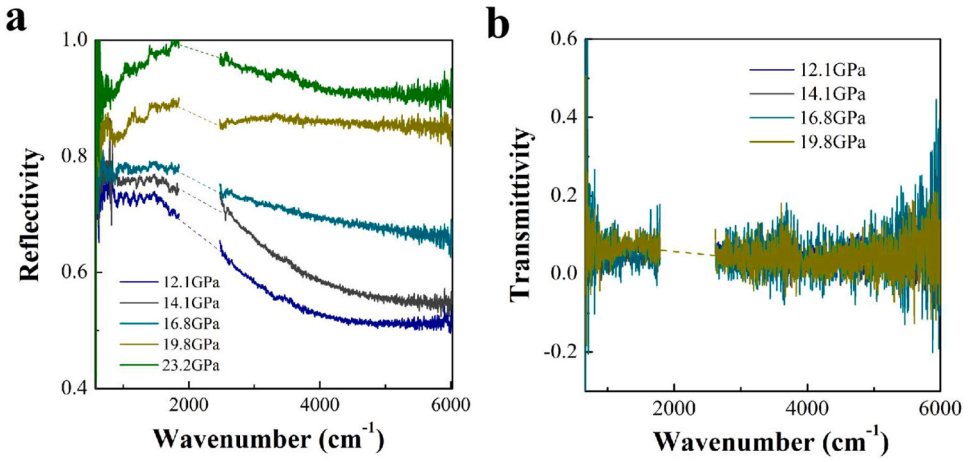

Fig. 3. Infrared spectra of Sb_2Te_3 from 12.1 GPa to 23.2 Gpa. (a) The pressure dependence of reflectivity at different pressure. (b) The pressure dependence of transmittivity at different pressure.

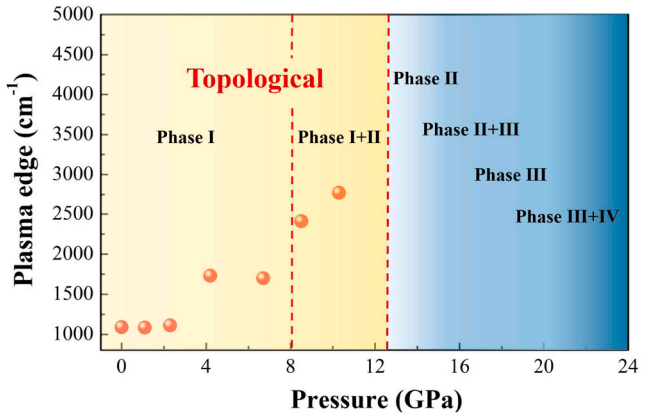

Fig. 4. Plasma edges and topological phase diagram of Sb_2Te_3 single crystals as a function of pressure.

and Sb_2Te_3 does not exhibit superconductivity up to a temperature of 1.5 K [11,37]. When the pressure was increased to 4.8 GPa, the plasma edges showed a jumping at 4.8 GPa. Corresponding to previous studies [11], a superconducting transition with a T_c of around 3 K was observed.

In addition, when pressure elevated to 8.5 GPa, the same plasma edge jumping occurs again, unlike 4.2 GPa, as the pressure increases, Sb_2Te_3 transforms from the P-type carrier to an N-type carrier, and a phase transition from phase I to phase II. As the pressure continue to increases, the position of plasma edges can no longer be observed in the mid-infrared. Our pressure-dependent IR spectroscopy results, as evidenced by the yellow portion of Fig. 4, reveal that Sb_2Te_3 loses its topological band structure when the plasma edge cannot be observed. While the plasma edge can still be observed in the region where phase I and phase II coexist. The plasma edge jumping at 4.2 GPa and 8.5 GPa corresponding to the reduction of band gap and phase transition. Previous studies have primarily concentrated on the modification of the peak resulting from the alteration of crystal structure under pressure [12,15,30,39–41]. However, there has been limited research on the plasma edge. Here, we can still find the relationship between the topological band structure changes of materials under pressure and the changes of plasma edges. In the high-pressure infrared experiment of Ag_2Se by zhao et al. [18], although plasma edges were not discussed, we found that the topological phase transition was also closely related to the change of plasma edges. Furthermore, there are unusual band structure alterations under pressure that are also closely associated with modifications in the plasma edges. Tran et.al. have determined the pressure dependence of the optical properties of giant Rashba spin splitting system BiTeI and the interband plasmon becomes overdamped above

9 GPa [34]. Combined with the change of Sb_2Te_3 plasma edges in this paper, it can clearly reflect the change of its carrier concentration and the disappearance of its topological structure. Therefore, in comparison to high-pressure Raman and XRD, high-pressure infrared spectra may be more effective in reflecting the characteristic properties of specific band structural materials.

We present the electronic structures calculated from theoretically optimized crystal structure since those referenced from experimental structure [42]. Fig. 5 illustrates band structures of Sb_2Te_3 with phase I and II. As shown in Fig. 5(a) and (c), the two opposite surfaces of Sb_2Te_3 are degenerate and exhibit a robust TIs electronic structure with their Fermi energy lying within the energy gap of Sb_2Te_3. It is clearly that the conduction band and valence band are main contributed by Sb and Te, respectively. The conduction band minima (CBM) is main contributed by Te and valence band maxima (VBM) is main contribute by Sb at Gamma point in the first Brillouin Zone, which is consistent with other calculations [11]. It indicates that the Sb_2Te_3 with phase I shows topological behavior. When the pressure rises to 12.1 GPa, Sb_2Te_3 transitions into phaseII(C2/m) [11,42], its band structures are shown in Fig. 5(b) and (d), respectively. Because of high pressure, in comparison with Fig. 5(a), the band gap is shifted from 0.13 eV to 0.10 eV, which resulting in the splitting of the energy level and spin polarization near the Fermi level. Its electronic transport properties can be considerably improved as a result of density of states at the Fermi level increases, which makes the transition of electrons from the valence band to the conduction band becomes easier. Unfortunately, there is no topological surface state in Phase II, which can be seen from Fig. 5(d). Supplementary Fig. S1 displayed band structure of Sb_2Te_3 for (a) phase I and (b) phase II without SOC. Compared with Fig. 5(d) and Supplementary Fig. S1(b), the band inversion is nearly vanished at Gamma point. In addition, the band structure of Phase III and phase VI is also calculated and shown in Supplementary Fig. S2. The energy gap is further reduced under increasing of pressure and the Fermi energy level enters to conduction band, showing a metallic behavior. Therefore, the results of theoretical calculation are consistent with our experimental observations.

In general, a measurement of reflectance over the appropriate frequency range can extract the optical constants and plasma frequency. The plasma frequency then affected by the ratio of carrier density to effective mass, n/m^*. In this paper, the pressure leads to the phase transition of crystal structure and modulation of Sb and Te atoms, which bring out the change of band dispersion relationship, directly result in the variations of n/m^* as the pressure changes. Therefore, we can clearly observe the relationship between the plasma edge and topological properties of Sb_2Te_3 under pressure.

4. Conclusion

To summarize, we have determined the pressure dependence of the infrared spectrum properties of Sb_2Te_3 as the pressure increases up to 23.2 GPa. The reflectivity and transmittivity exhibit significant variations under pressure. As pressure increases, the band gap monotonically decreases, while the reflectivity increases. In the reflectivity infrared spectra, we observe a plasma edge jump at 4.2 GPa, which is attributed to the pressure-induced carrier density changes in Sb_2Te_3. When the pressure reach to 8.5 GPa, the plasma edges exhibit a further jump. The jumping is not solely due to the transition from p-type to n-type characteristics but also involves the emergence of a new phase of Sb_2Te_3 (Phase I+II). Until the pressure reach to 12.3 GPa, the mixed I+ II phase disappears. Moreover, by analyzing the modification of plasma edges under pressure, we discover that the disappearance of plasma edges under high pressure corresponds to the disappearance of topological band structure. Under standard experiment measures, it is difficult to find effective means to react topological bands under high pressure, except through theoretical calculations. Perhaps under high pressure, high pressure plasma edge can essentially reflect the characteristic

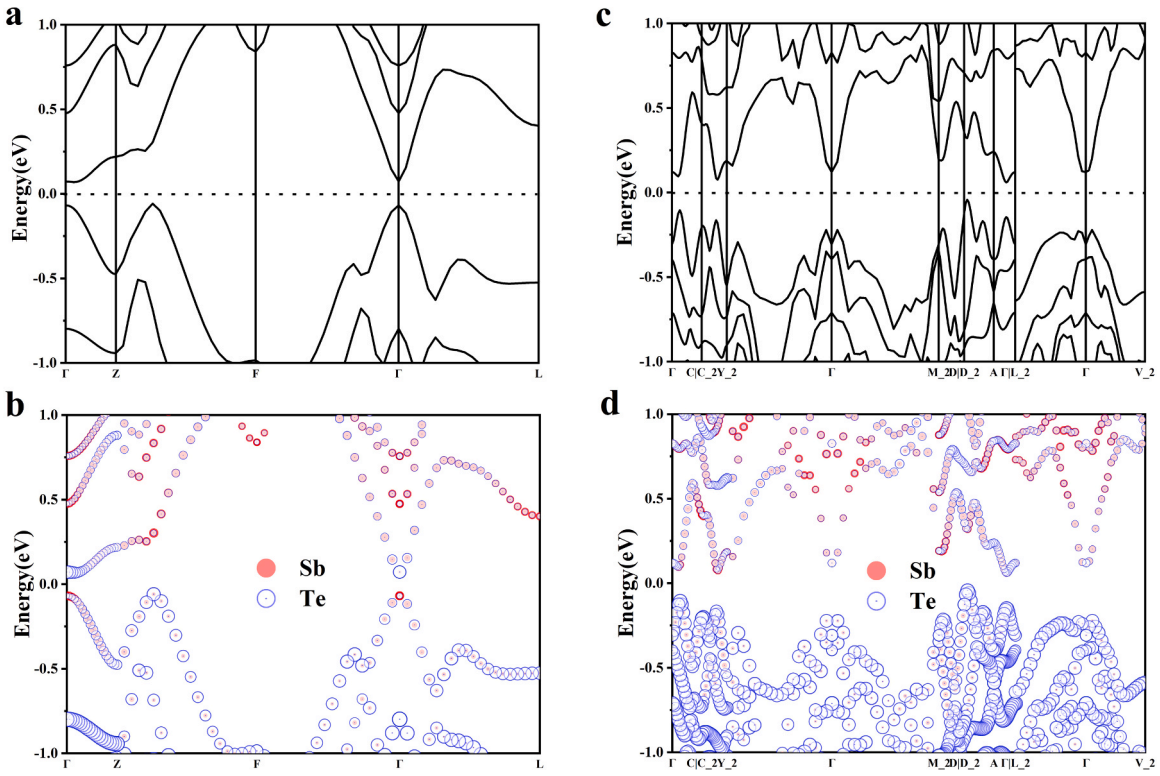

Fig. 5. Band structure of Sb_2Te_3 for (a) phase I and (b) phase II with SOC. Projected band structure of Sb_2Te_3 for (c) phase I and (d) phase II with SOC, the size of circle indicates the magnitude of the projection on Sb and Te element, the red circle represents Sb atom and blue circle represents Te atom. The dash line is the Fermi energy.

properties of certain special band structural materials.

CRediT authorship contribution statement

Zhang Sa: Data curation, Writing – review & editing. **Hu Bin:** Writing – original draft, Writing – review & editing. **Wang Xi:** Data curation. **Yu Xiaohui:** Funding acquisition, Writing – review & editing. **Jin Changqing:** Funding acquisition, Writing – review & editing. **Gao Chan:** Data curation. **Zhang ZeXiao:** Data curation. **Wang Chun:** Data curation. **Zheng Xu:** Data curation, Formal analysis, Funding acquisition, Writing – original draft, Writing – review & editing.

Declaration of Competing Interest

The authors declare that they have no known competing financial interests or personal relationships that could have appeared to influence the work reported in this paper.

Data Availability

No data was used for the research described in the article.

Acknowledgments

This study were partially supported by Sichuan Science and Technology Program (No.2023NSFSC1371, No.2023NSFSC1337, No.2022NSFSC0332) and Chengdu University of Technology 2023 Young and Middle-aged Backbone Teachers Development Funding Program (No. 10912-JXGG2023-09014). We are grateful for Synergic Extreme Condition User Facility (SECUF).

Appendix A. Supporting information

Supplementary data associated with this article can be found in the online version at doi:10.1016/j.jallcom.2024.173500.

References

[1] G. Harari, M.A. Bandres, Y. Lumer, M.C. Rechtsman, Y.D. Chong, M. Khajavikhan, D.N. Christodoulides, M. Segev, Topological insulator laser: theory, Science 359 (2018) 4003.
[2] I. Appelbaum, H.D. Drew, M.S. Fuhrer, Proposal for a topological plasmon spin rectifier, Appl. Phys. Lett. 98 (2011), 023103-1.
[3] S. Julià-Farré, M. Müller, M. Lewenstein, A. Dauphin, Interaction-induced polarons and topological defects in a topological Mott insulator, Phys. Rev. Lett. 125 (2020) 240601.
[4] Y. Ma, G. Liu, P. Zhu, H. Wang, X. Wang, Q. Cui, J. Liu, Y. Ma, Determinations of the high-pressure crystal structures of Sb_2Te_3, J. Phys. Condens. Matter 24 (2012) 475403.
[5] A. Mavlonov, T. Razykov, F. Raziq, J. Gan, L. Qiao, A review of Sb_2Se_3 photovoltaic absorber materials and thin-film solar cells, Sol. Energy 201 (2020) 227–246.
[6] K. Lee, Y.I. Jhon, S. Kwon, G. Lim, J. Kim, J.H. Lee, Nonlinear optical properties of tin telluride topological crystalline insulator at a telecommunication wavelength, J. Alloy. Compd. 925 (2022) 166643.
[7] K. Mazumder, P.M. Shirage, A brief review of Bi2Se3 based topological insulator: from fundamentals to applications, J. Alloy. Compd. 888 (2021) 161492.
[8] B.Q. Lv, T. Qian, H. Ding, Experimental perspective on three-dimensional topological semimetals, Rev. Mod. Phys. 93 (2021) 025002.
[9] Z.C. Rao, H. Li, T.T. Zhang, S.J. Tian, C.H. Li, B.B. Fu, C.Y. Tang, L. Wang, Z.L. Li, W.H. Fan, J.J. Li, Y.B. Huang, Z.H. Liu, Y.W. Long, C. Fang1, H.M. Weng, Y.G. Shi, H.C. Lei, Y.J. Sun, T. Qian, H. Ding, Observation of unconventional chiral fermions with long Fermi arcs in CoSi, Nature 567 (2019) 496–499.
[10] S.Y. Gao, S. Xu, H. Li, C.J. Yi, S.M. Nie, Z.C. Rao, H. Wang, Q.X. Hu, X.Z. Chen, W. H. Fan, J.R. Huang, Y.B. Huang, N. Pryds, M. Shi, Z.J. Wang, Y.G. Shi, T.L. Xia, T. Qian, H. Ding, Time-reversal symmetry breaking driven topological phase transition in EuB_6, Phys. Rev. X 11 (2021) 021016.
[11] J. Zhu, J.L. Zhang, P.P. Kong, S.J. Zhang, X.H. Yu, J.L. Zhu, Q.Q. Liu, X. Li, R.C. Yu, R. Ahuja, W.G. Yang, G.Y. Shen, H.K. Mao, H.M. Weng, X. Dai, Z. Fang, Y.S. Zhao, C.Q. Jin, Superconductivity in topological insulator Sb_2Te_3 induced by pressure, Sci. Rep. 3 (2013) 1–6.
[12] P.P. Kong, F. Sun, L.Y. Xing, J. Zhu, S.J. Zhang, W.M. Li, Q.Q. Liu, X.C. Wang, S. M. Feng, X.H. Yu, J.L. Zhu, R.C. Yu, W.G. Yang, G.Y. Shen, Y.S. Zhao, R. Ahuja, H. K. Mao, C.Q. Jin, Superconductivity in strong spin orbital coupling compound Sb_2Se_3, Sci. Rep. 4 (2014) 6679.
[13] A. Akrap, M. Tran, A. Ubaldini, J. Teyssier, E. Giannini, D. van der Marel, P. Lerch, C.C. Homes, Optical properties of Bi2Te2Se at ambient and high pressure, Phys. Rev. B 23 (2012) 235207.
[14] Y. Wang, Y. Ma, G. Liu, J. Wang, Y. Li, Q. Li, J. Zhang, Y. Ma, G. Zou, Experimental observation of the high pressure induced substitutional solid solution and phase transformation in Sb_2S_3, Sci. Rep. 8 (2018) 14795.
[15] A. Irizawa, K. Sato, M. Kobayashi, K. Shimai, T. murakami, H. Okamura, T. Nanba, M. Matsunami, H. Sugawara, H. Sato, Electronic state of $PrFe_4P_{12}$ under high pressure probed by infrared spectroscopy, Phys. B-Condens. Matter 403 (2008) 948–949.
[16] M.S. Bahramy, B.J. Yang, R. Arita, N. Nagaosa, Emergence of non-centrosymmetric topological insulating phase in BiTeI under pressure, Nat. Commun. 3 (2012) 679.
[17] R. Li, G. Liu, Q. Jing, X. Wang, H. Wang, J. Zhang, Y. Ma, Pressure-induced superconductivity and structural transitions in topological insulator SnBi2Te4, J. Alloy. Compd. 900 (2022) 163371.
[18] Z. Zhao, S. Wang, A.R. Oganov, P. Chen, Z. Liu, W.L. Mao, Tuning the crystal structure and electronic states of Ag_2Se: structural transitions and metallization under pressure, Phys. Rev. B 89 (2014) 180102.
[19] P.D. Pietro, F.M. Vitucci, D. Nicoletti, L. Baldassarre, P. Calvani, R. Cava, Y.S. Hor, U. Schade, S. Lupi, Optical conductivity of bismuth-based topological insulators, Phys. Rev. B, Condens. Matter 86 (2012) 045439.
[20] S.V. Dordevic, M.S. Wolf, N. Stojilovic, H. Lei, C. Petrovic, Signatures of charge inhomogeneities in the infrared spectra of topological insulators Bi_2Se_3, Bi_2Te_3 and Sb_2Te_3, J. Phys. Condens. Matter 25 (2013), 075501-075501.
[21] U. Dutta, S. Sahoo, P.S. Malavi, F. Piccirilli, P. Di Pietro, A. Perucchi, S. Lupi, S. Karmakar, Infrared spectroscopic measurements of structural transition and charge dynamics in 1T-$TiTe_2$ under pressure, Phys. Rev. B, Condens. Matter Mater. Phys. 99 (2019), 125105.1-125105.8.
[22] Y.D. Hai, Wakabayashi, K.I.C.F. Nanoarchitechtonics, N.I.F.M. Sci, Tsukuba, N.I.F. M. Science, I.C.F.M. Nanoarchitechtonics, Namiki, J.W.K.N. Jp, Retardation effects on plasma waves in graphene, topological insulators, and quantum wires, Phys. Rev. B 92 (2000) 045434.
[23] S. Raghu, S.C. Zhang, S.B. Chung, Collective modes of a helical liquid, Phys. Rev. Lett. 104 (2010) 1–4.
[24] I. Appelbaum, H.D. Drew, M.S. Fuhrer, Proposal for a topological plasmon spin rectifier, Appl. Phys. Lett. (2) (2010) 023103.
[25] G. Siroki, D.K.K. Lee, P. D.Haynes, V. Giannini, Single-electron induced surface plasmons on a topological nanoparticle, Nat. Commun. 7 (2015) 12375.
[26] F. Ye, C.X. Liu, Plasmon modes in magnetically doped single-layer and multilayer helical metals, Phys. Rev. B Condens. Matter 87 (2013) 269–275.
[27] P. Di Pietro, M. Ortolani, O. Limaj, A. Di Gaspare, V. Giliberti, F. Giorgianni, M. Brahlek, N. Bansal, N. Koirala, S. Oh, Observation of Dirac plasmons in a topological insulator, Nat. Nanotechnol. 8 (2013) 556.
[28] L.L. Li, W. Xu, Surface plasmon polaritons in a topological insulator embedded in an optical cavity, Appl. Phys. Lett. 104 (2014) 146802.
[29] B.A. Bernevig, T.L. Hughes, Quantum spin Hall effect and topological phase transition in HgTe quantum wells, Science 314 (2006) 1757–1761.
[30] L.J. Zhang, J.S. Zhang, M.H. Weng, Zhang, X.L. Yang, Pressure-induced superconductivity in topological parent compound Bi_2Te_3, Appl. Phys. Sci. 108 (2011) 24–28.
[31] A. Akrap, M. Tran, A. Ubaldini, J. Teyssier, E. Giannini, D.V.D. Marel, P. Lerch, C. C. Homes, Optical properties of Bi_2Te_2Se at ambient and high pressure, Phys. Rev. B 86 (2012) 235207.
[32] G. Kresse, J. Hafner, Ab inito molecular-dynamics for liquid-metals, Phys. Rev. B 47 (1993) 558.
[33] G. Kresse, J. Furthmiiller, Efficiency of ab-initio total energy calculations for metals and semiconductors using a plane-wave basis set, Comput. Mater. Sci. 6 (1996) 15.
[34] Dressel, Electrodynamics of Solids, Cambridge University Press, 2002.
[35] Akinori Irizawa, Kazuyuki Sato, Masayo Kobayashi, Koutarou, Electronic state of $PrFe_4P_{12}$ under high pressure probed by infrared spectroscopy, Phys. B Condens. Matter 403 (2008) 948–949.
[36] M.K. Tran, J. Levallois, P. Lerch, J. Teyssier, A.B. Kuzmenko, G. Autès, O. V. Yazyev, A. Ubaldini, E. Giannini, D. van der Marel, A. Akrap, Infrared- and Raman-spectroscopy measurements of a transition in the crystal structure and a closing of the energy gap of BiTeI under pressure, Phys. Rev. Lett. 112 (2014), 047402-047402.
[37] O. Gomis, R. Vilaplana, F.J. Manjón, P. RodríguezHernández, E. PérezGonzález, A. Muñoz, V. Kucek, C. Drasar, Lattice dynamics of Sb_2Te_3 at high pressures, Phys. Rev. B 84 (2011) 1160–1164.
[38] J. Zhao, H. Liu, L. Ehm, Z. Chen, G. Gu, Pressure-induced disordered substitution alloy in Sb_2Te_3, Inorg. Chem. 50 (2011) 11291–11293.
[39] A. Hushur, M.H. Manghnani, H. Werheit, P. Dera, Q. Williams, High-pressure phase transition makes $B_{4.3}C$ boron carbide a wide-gap semiconductor, J. Phys. Condens. Matter 28 (2016) 045403.
[40] H. Takizawa, K. Uhcda, M. Shimada, High pressure phase transition of $CrSb_2$, Rev. High. Press. Sci. Technol. 7 (2009) 1043–1045.
[41] A. Jayaraman, B. Batlogg, L.G. Vanuitert, High-pressure Raman study of alkaline-earth tungstates and a new pressure-induced phase transition in $BaWO_4$, Phys. Rev. B 28 (1983) 4774.
[42] J. Zhao, H.Z. Liu, L. Ehm, Z.Q. Chen, S. Sinogeikin, Y.S. Zhao, G. Gu, Pressure induced disordered substitution alloy in Sb2Te3, Inorg. Chem. 50 (2011) 11291–11293.